energies

MDPI

Communication

Nano-Fe_3O_4/Carbon Nanotubes Composites by One-Pot Microwave Solvothermal Method for Supercapacitor Applications

Sul Ki Park [1,*], Jagadeesh Sure [2], D. Sri Maha Vishnu [3], Seong Jun Jo [4], Woo Cheol Lee [4], Ibrahim A. Ahmad [5] and Hyun-Kyung Kim [4,*]

1 Department of Engineering, University of Cambridge, Cambridge CB3 0FS, UK
2 Department of Physics, School of Advanced Sciences, Vellore Institute of Technology (VIT) University, Vellore TN-632014, India; jagadeesh.sure@vit.ac.in
3 Department of Materials Science and Metallurgy, University of Nizwa, Birkat Al Mouz 616, Nizwa, Oman; vishnu@unizwa.edu.om
4 Department of Materials Science and Engineering, Kangwon National University, Chuncheon 24341, Korea; runs7777@kangwon.ac.kr (S.J.J.); xndos63@kangwon.ac.kr (W.C.L.)
5 Department of Materials Science and Metallurgy, University of Cambridge, Cambridge CB3 0FS, UK; ibrahim-ahmad@larnsen.com
* Correspondence: sp991@cam.ac.uk (S.K.P.); hkk@kangwon.ac.kr (H.-K.K.); Tel.: +44-(0)-78-564109 (S.K.P.); +82-(0)-33-250-6264 (H.-K.K.)

Abstract: Carbon nanotubes (CNTs) are being increasingly studied as electrode materials for supercapacitors (SCs) due to their high electronic conductivity and chemical and mechanical stability. However, their energy density and specific capacitance have not reached the commercial stage due to their electrostatic charge storage system via a non-faradic mechanism. Moreover, magnetite (Fe_3O_4) exhibits higher specific capacitance originating from its pseudocapacitive behaviour, while it has irreversible volume expansion during cycling. Therefore, a very interesting and facile strategy to arrive at better performance and stability is to integrate CNTs and Fe_3O_4. In this study, we demonstrate the microwave-solvothermal process for the synthesis of Fe_3O_4 nanoparticles uniformly grown on a CNT composite as an electrode for SCs. The synthesized Fe_3O_4/CNT composite delivers a reversible capacitance of 187.1 F/g at 1 A/g, superior rate capability by maintaining 61.6% of 10 A/g (vs. 1 A/g), and cycling stability of 80.2% after 1000 cycles at 1 A/g.

Keywords: supercapacitor; carbon nanotube; iron oxide; microwave-solvothermal process; composite

Citation: Park, S.K.; Sure, J.; Vishnu, D.S.M.; Jo, S.J.; Lee, W.C.; Ahmad, I.A.; Kim, H.-K. Nano-Fe_3O_4/Carbon Nanotubes Composites by One-Pot Microwave Solvothermal Method for Supercapacitor Applications. *Energies* **2021**, *14*, 2908. https://doi.org/10.3390/en14102908

Academic Editor: Bahman Shabani

Received: 31 March 2021
Accepted: 12 May 2021
Published: 18 May 2021

1. Introduction

Supercapacitors (SCs) are promising energy storage devices owing to their long cycle stability, superior power density, and fast charge/discharge [1–8]. It results from the effective charge storage process through the ion adsorption/desorption at the electrical double layer onto the electrode surface.

Carbon nanotubes (CNTs) have attracted much attention as an electrode for SCs, where the charge can be electrostatically stored with non-faradic reaction, because of their good chemical stability, high mechanical strength, and excellent electrical conductivity [9–13]. However, the use of CNTs materials as commercial electrodes is limited due to their low specific capacitance originating from the non-faradic process, which requires further enhancement in the specific capacitance [9–13].

To overcome this limitation, one promising approach is the use of metal oxides as an electrode. The metal oxide electrode can store charges by the faradic redox reaction, which shows higher specific capacitance, called pseudocapacitance [14–18]. Especially, magnetite (Fe_3O_4) has gained significant attention as a pseudocapacitive electrode owing to its large theoretical capacitance, natural abundance, low cost, and eco-friendliness [19–23].

However, the continuous charging and discharging process of Fe_3O_4 can lead to irreversible volume change, resulting in severe electrochemical performance decay. Therefore, the modification of the Fe_3O_4-based electrode is important to satisfy the high capacitance, stable cycling performance, and superior rate capability required for SCs.

A desirable approach to resolve these problems is the incorporation of redox-active Fe_3O_4 nanoparticles into the electrically conductive CNT matrix. This approach can offer enhanced specific capacitance while preserving cycling stability and rate capability. The fabrication of Fe_3O_4/CNT hybrid structure with uniform nanoparticles is challenging as it requires a complicated process including multi- and time-consuming steps and the use of dangerous chemical reagents. Thus, developing a simple and eco-friendly synthesis strategy to enhance the electrochemical performance of electrode materials is crucial.

Herein, we report the synthesis of a well-designed Fe_3O_4/CNT structure using a straightforward strategy relying on a simple microwave-solvothermal method, where CNT serves as an effective heating template for facilitating nucleation of Fe_3O_4 nanoparticles. Uniform Fe_3O_4 nanoparticles with high purity were deposited onto the surface of CNTs using the microwave-solvothermal process. The synthesized Fe_3O_4/CNT architecture shows high specific capacitance, rate capability, and good cycling performances.

2. Materials and Methods

The nano-Fe_3O_4/CNTs composite was synthesized following the microwave solvothermal method. CNTs (0.1 g) were sonicated in diethylene glycol (DEG, >99%, Fluka, 70 mL). Subsequently, $FeCl_2$ $4H_2O$ (0.207 g, Aldrich), $FeCl_3$ $6H_2O$ (0.507 g, Junsei), ammonium hydroxide (15 mL, 30 wt %, Junsei), and sodium acetate (1.32 g, Sigma Aldrich) were included in the solution, which was then loaded into 100 mL Teflon vessels sealed and placed in a microwave system (MARS-5, CEM Corporation). The reaction mixture was heated to 180 °C where it was maintained at that temperature for 10 min. Then, the mixture was naturally cooled down to room temperature.

A field-emission scanning electron microscopy (FE-SEM; JEOL 6340F) and a transmission electron microscopy (TEM; 200 kV; CM200, Philips) were used to analysed the surface morphology and structure of the nano-Fe_3O_4/CNTs composites, respectively. The structural properties were studied by performing powder X-ray diffraction (XRD) measurements (Rigaku, Japan). Moreover, an X-ray photoelectron spectroscopy (XPS; 15 kV, 150 W; ESCALAB 250, Thermo Electron Corporation) was used to evaluate the surface chemistry of nano-Fe_3O_4/CNTs, and a thermogravimetric analyser (TGA, STA 409 PC, Netzsch) allowed to conduct thermo-gravimetric studies using a ramp rate of 10 °C/min in air atmosphere from room temperature to 800 °C.

For the electrochemical test, the slurry was made with 80 wt.% active materials (nano-Fe_3O_4-CNT), 10 wt.% conductive additives (Super-P), and 10 wt.% binder (Polyvinylidene fluoride) using 1-methyl pyrrolidone and cast with active mass loading of 1–1.3 mg/cm^2 (Platinum substrate). Electrochemical tests, including cyclic voltammogram (CV) and galvanostatic charge–discharge (GCD) curves, were conducted using a potentiostat (Biologics VMP3) and a 1 M Na_2SO_3 solution in a −1.0–0 V potential window vs. SCE. The mass of the nano-Fe_3O_4/CNT composite was used to normalize the current response in the CV and GCD curves. The respective specific capacitances (Cs) were determined by using half integrated area of the GCD curve to obtain the charge (Q) and subsequently dividing the charge by the mass of the electrode (m) and the width of the potential window (ΔV) following equation: $Cs = Q/m\ \Delta V$.

3. Results and Discussion

In the nano-Fe_3O_4/CNT composite development, the CNTs functioned as a template for the selective heterogeneous nucleation and growth of Fe_3O_4 nanoparticles. In particular, the carbonaceous materials absorb the microwave energy, converting it into heat to provide a high temperature on the surface of CNTs relative to the solution. In general, because the nucleation of metal ions occurs on hot spots, the Fe_3O_4 precursor in the solution is

considered to be selectively nucleated and uniformly grown on the surface of the CNTs, as shown schematically in Figure 1. Additionally, the microwave-solvothermal method could favour the process owing to its distinct advantages over conventional hydrothermal or solvothermal methods, such as lower synthesis temperature, higher reaction rate, shorter reaction time, and smaller resulting particles [24,25].

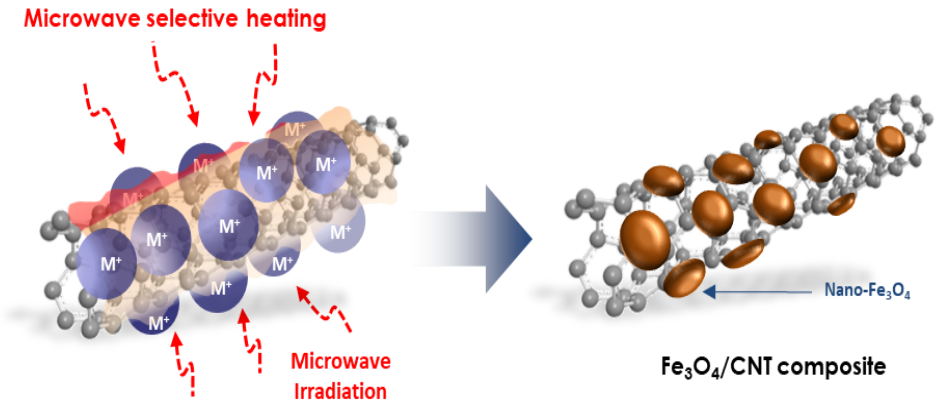

Figure 1. Schematic illustration of formation of the nano-Fe_3O_4/CNT composite using microwave solvothermal process.

The morphologies of the Fe_3O_4/CNT composite obtained from the microwave-solvothermal method were characterized using SEM and TEM, shown in Figure 2, Figures S1 and S2 (Supplementary Materials). SEM and low-magnification TEM images show that the iron oxide nanoparticles grew properly onto CNT bundles with a diameter of approximately 25 nm (Figures 2a–c and S2a,b). The selected area electron diffraction (SAED) pattern of Fe_3O_4/CNT exhibits distinct diffraction rings corresponding to the (440), (400), (311), and (220) crystalline planes of Fe_3O_4, identifying that the highly crystalline Fe_3O_4 nanoparticles grew on the CNT (Figure 2d) [19,26,27]. As shown in Figure 2e, the TEM image displays the size of iron oxide nanoparticles grown uniformly on CNT ranges from 2 to 4 nm. Such a uniform distribution of iron oxide particles of nano-Fe_3O_4/CNT originated from dissolution and precipitation of the iron oxide precursor on the surface of CNTs during the microwave-solvothermal process. In addition, a high magnification TEM image of Fe_3O_4/CNT composite shows the formation of a crystalline pattern with a d-spacing of 0.251 nm, which corresponds to the (311) plane of Fe_3O_4.

Figure 3a shows the XRD patterns of the bare CNT and Fe_3O_4/CNT composite. The observed XRD peaks for Fe_3O_4/CNT at 18.4, 35.6, 43.3, 47.4, 57.2, 62.8, and 66.1° are assigned to the (111), (220), (311), (400), (442), (511), and (440) planes, respectively. These results match well with the magnetite Fe_3O_4 (JCPDS card No. 19-629) [19,26,27]. The XRD pattern for Fe_3O_4/CNT also shows the presence of CNT, which was clearly confirmed from the broad peak of (200) located at 25.4°. As mentioned previously, the major peak corresponding to the (311) plane shown in the XRD pattern matches very well with the observed lattice fringe spacing of 0.251 nm for the Fe_3O_4 crystalline phase (Figures 2f and 3a).

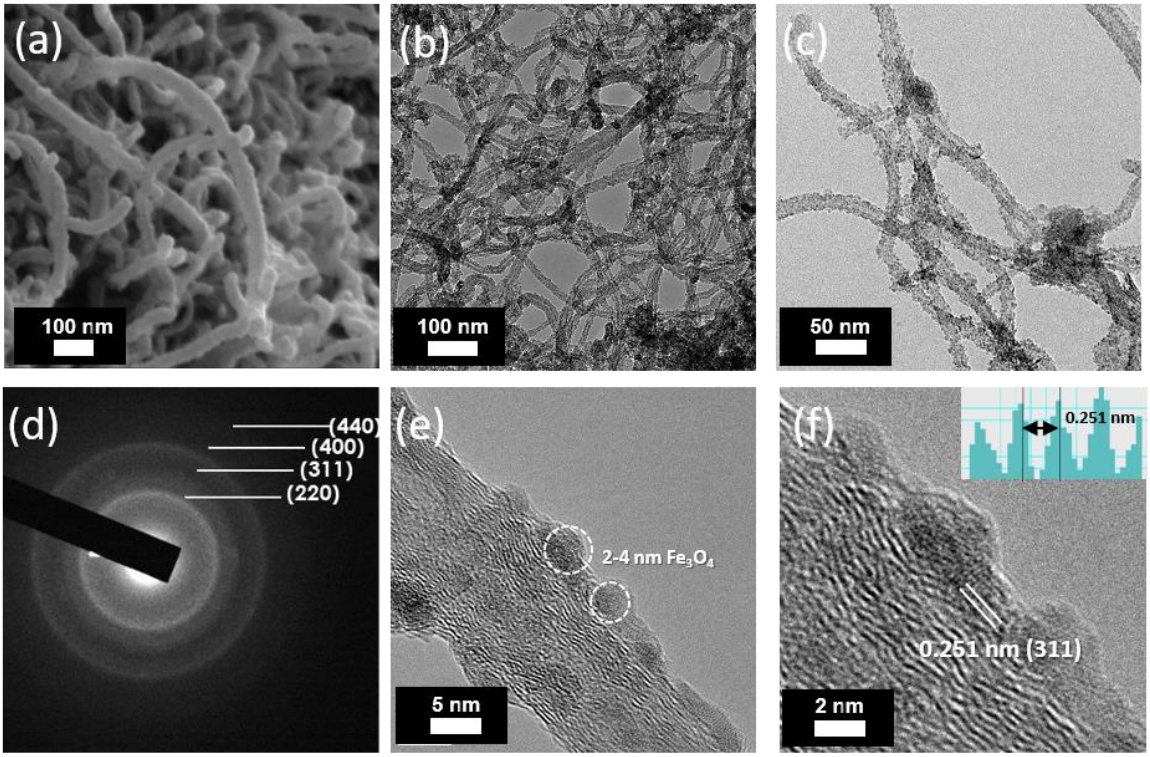

Figure 2. (**a**) SEM image (**b**,**c**) TEM images. (**d**) Selected area electron diffraction pattern or SAED pattern, (**e**,**f**) FE-TEM images of nano-Fe_3O_4/CNT composite.

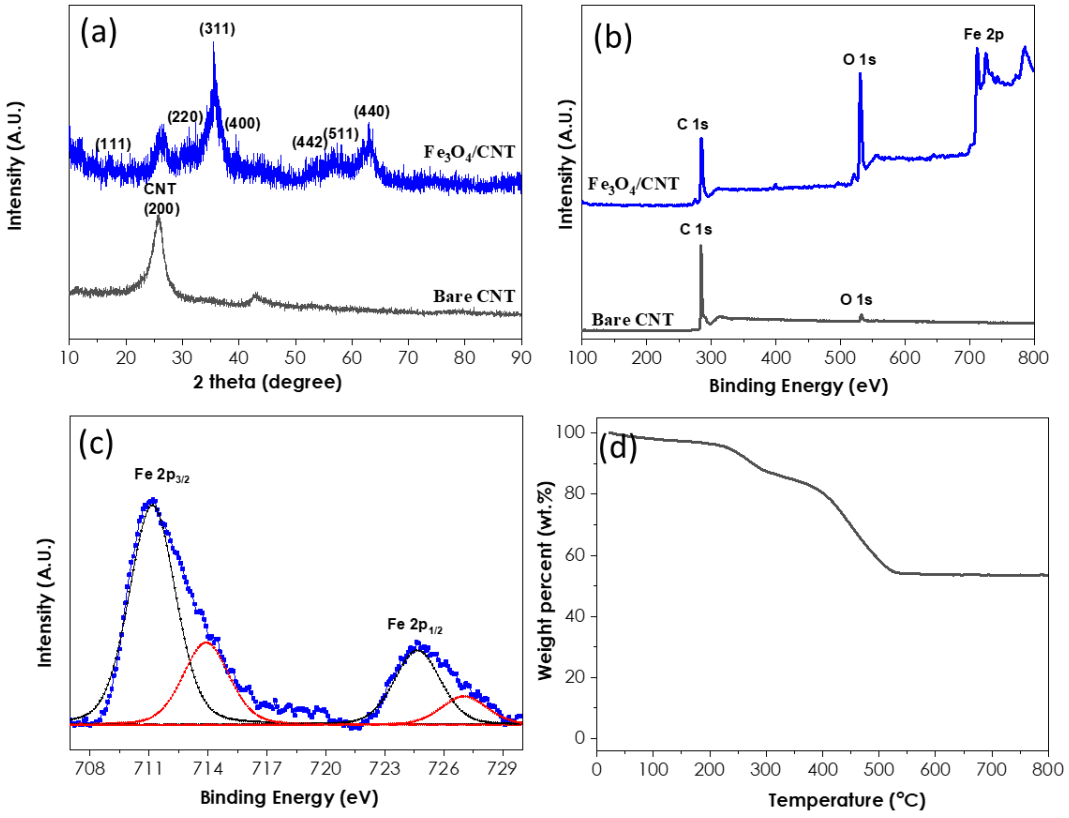

Figure 3. (**a**) XRD patterns and (**b**) XPS survey spectra of bare CNT and nano-Fe_3O_4/CNT composite and (**c**) high-resolution XPS spectrum of Fe 2p collected from Fe_2O_3-CNT composite. (**d**) TGA curve of nano-Fe_3O_4/CNT composite.

The chemical properties such as composition and bonding nature of Fe_3O_4/CNT composite are characterized by XPS analysis (Figure 3b,c). The full-scale XPS spectra for Fe_3O_4/CNT exhibit C1s and O1s at 285.4 eV and 529.1 eV, as shown in Figure 3b. In addition, the peaks centred at 710 eV and 725 eV assigned to the Fe $2p_{3/2}$ and Fe $2p_{1/2}$ states (Figure 3c) corresponded to the Fe_3O_4 of nano-Fe_3O_4/CNTs [24]. Note that the peaks of Fe $2p_{1/2}$ are detected at approximately 724.5 eV and 727.0 eV, respectively, indicating the formation of mixed oxides of Fe (II) and Fe (III). Moreover, the peak of Fe $2p_{3/2}$ comprises two peaks at approximately 711.1 eV and 713.9 eV, respectively, which further confirm the formation of Fe_3O_4 [28]. The results clearly indicate the successful formation of Fe_3O_4 nanoparticles on CNT by the microwave-solvothermal method. XPS results also emphasize the high purity of the prepared Fe_3O_4/CNT composite and the absence of any impurities. The TGA measurement was conducted to determine the actual mass of Fe_3O_4 nanoparticles in the Fe_3O_4/CNT composite. The results (Figure 3d) show that the synthesized Fe_3O_4/CNT composite accommodated 55 wt.% Fe_3O_4.

The electrochemical performance of the Fe_3O_4/CNT composite was analysed through the capacitor performances relying on the CV and GCD measurements in a three-electrode cell, as shown in Figure 4. An amount of 1 M Na_2SO_3 electrolyte was used as the electrolyte within a potential range of −1.0–0 V. Figure 4a,b show the CV of Fe_3O_4/CNT composite measured with scan rates of 5, 10, 20, 30, 40, 100, 200, and 300 mV/s. The horizontal line representing the CV curves of the bare Pt-substrate in Figure S3 implies that no capacitance associated with the used Pt-substrate is present. CV curves of Fe_3O_4/CNT composite electrodes present a rectangular and symmetrical shape with redox peaks, which is indicative of the combined contribution of the double layer capacitive and pseudocapacitive behaviours from CNT and Fe_3O_4, respectively. The pseudocapacitive reaction mechanism of Fe_3O_4 in 1 M Na_2SO_3 electrolyte is based on the reversible redox reactions between Fe^{2+} and Fe^{3+} accompanied with the intercalation of SO_3^{2-} ions from electrolyte [23,29,30]:

$$\begin{aligned} FeO + SO_3^{2-} &\leftrightarrow FeSO_4 + 2e^- \\ 2Fe^{II}O + SO_3^{2-} &\leftrightarrow (Fe^{III}O) + SO_3^{2-}(Fe^{III}O) + 2e^- \end{aligned} \quad (1)$$

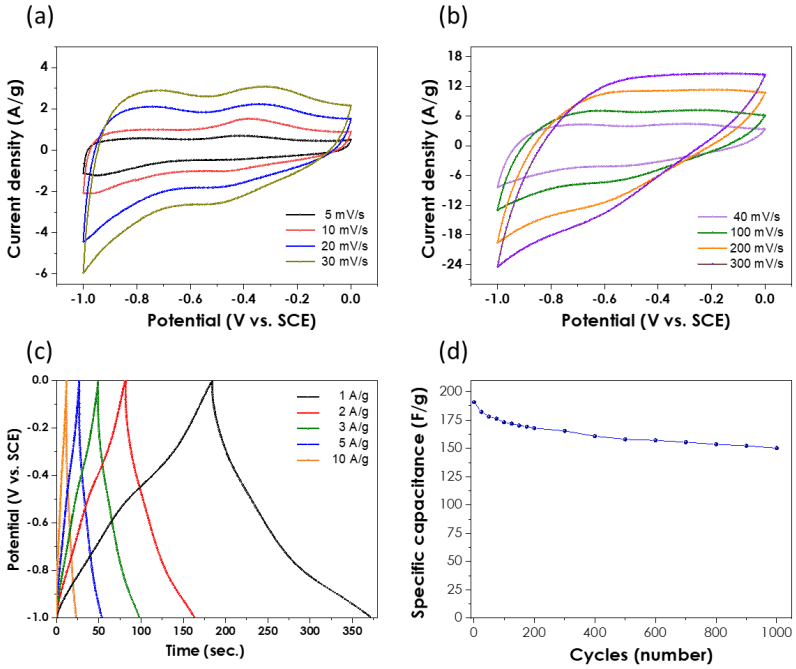

Figure 4. Cyclic voltammograms at scan rates of (**a**) 5–30 mV/s, (**b**) 40–300 mV/s, (**c**) charge–discharge curves (current density: 1–10 A/g), and (**d**) cycling performance of the nano-Fe_3O_4/CNT composite electrode (1 A/g) (electrolyte: 1 M Na_2SO_3).

The b values were derived from the cathodic and anodic peaks for CV curves of the Fe_3O_4/CNT composite using log(i) vs. log(v) plots (Figure S4a).

$$\log (i) = b \log (v) + \log (a), \quad (2)$$

where a and b are constants determined by the intercept and slope of the log(i)–log(v) plots, respectively. The b-value of 0.5 indicates a diffusion-controlled behaviour, whereas the value of 1 indicates a surface pseudocapacitance-dominated behaviour. The b-values of the cathodic peak, anodic peak 1, and anodic peak 2 for Fe_3O_4/CNT composite are 0.977, 0.975, and 0.833, respectively, implying a pseudocapacitive-controlled behaviour (Figure S4b).

Fe_3O_4/CNT composite curves retain a similar shape with distinct and reversible redox peaks as the scan rate increased from 5 to 300 mV/s. The specific capacitance of Fe_3O_4/CNT composite was also calculated from the GCD curves (Figure 4c) as 187.1, 163.3, 145.9, 132.6, and 115.4 F/g at current densities of 1, 2, 3, 5, and 10 A/g, respectively. The calculated specific capacitances of Fe_3O_4/CNT composite are higher than that of pristine CNTs (~50 F/g) [30]. Our synthesized Fe_3O_4/CNT composite has the superior specific capacitance compared to those measured in a sodium-based electrolyte such as Na_2SO_3 and Na_2SO_4 reported in previous studies [24,27,30,31]. This result was due to the uniform Fe_3O_4 nanoparticles grown on CNTs that effectively improved the capacitive behaviour of CNT by adding a pseudocapacitive reaction. The GCD curves of Fe_3O_4/CNT still remained symmetric and exhibited high specific capacitance even at the high current density of 10 A/g, suggesting good rate capability with superior reversibility. These results are consistent with those from CV curves. High rate capability results from the highly electronic conductive CNT matrix, as it provides a practical pathway for fast ion/electron transport.

Besides the rate performance, the cycle stabilities of the Fe_3O_4/CNT composite electrode are evaluated at a current density of 1 A/g (Figure 4d). The specific capacitance of Fe_3O_4/CNT composite was measured as 150 F/g after 1000 cycles, showing high capacitance retention of 80.2%. The loss of specific capacitance that was approximately 20% might be due to the inevitable pulverization arising from the volume expansion of Fe_3O_4 particles. However, this implies that the conductive CNT matrix and the strong connection between CNT and Fe_3O_4 nanoparticles could reduce the drastic volume expansion during the charge and discharging process, which is beneficial for good cycle stability. The excellent capacitor performance of the Fe_3O_4/CNT composite can be due to the synergistic effect between the high pseudocapacitive Fe_3O_4 and the superior electronic conductive carbon matrix.

4. Conclusions

In summary, we synthesized a nano-Fe_3O_4/CNT structured electrode consisting of uniform Fe_3O_4 particles' growth on the CNT matrix to enhance the specific capacitance, rate capability, and cycle stability of Fe_3O_4 for SCs. Superior electrochemical performances of Fe_3O_4/CNT composite are attributed to the combined contribution from Fe_3O_4 nanoparticle and CNT matrix: (i) Fe_3O_4 nanoparticles showed a pseudocapacitive behaviour originating from the redox reactions with SO_3^{2-} ions and iron oxides. (ii) Excellent electroconductive CNT provided fast ion/electron transport and robust electrode structure with the double layer capacitive behaviour.

Supplementary Materials: The following are available online at https://www.mdpi.com/article/10.3390/en14102908/s1, Figure S1: TEM images of bare CNTs, Figure S2: SEM images of nano-Fe_3O_4/CNT composite, Figure S3: Cyclic voltammograms of Pt substrate, Figure S4: (a) Cyclic voltammograms at scan rates of 5–40 mV/s and (b) log(i) vs. log(v) plots at cathodic and anodic peaks of Fe_3O_4/CNT composite., Table S1, Comparison of the electrochemical performance of Fe_3O_4/carbon composite.

Author Contributions: S.K.P. and H.-K.K. designed the materials and experiments. S.K.P. and H.-K.K. fabricated the materials and performed the electrochemical characterisation. J.S., D.S.M.V., S.J.J., W.C.L., and I.A.A. participated in the electrochemical evaluations and structural characterisation. All authors have read and agreed to the published version of the manuscript.

Funding: This research received no external funding.

Institutional Review Board Statement: Not applicable.

Informed Consent Statement: Not applicable.

Data Availability Statement: Not applicable.

Acknowledgments: This study was supported by 2020 Research Grant from Kangwon National University and also supported by the National Research Foundation of Korea (NRF) grant-funded by the Korea government (MSIT) (No. 2020R1G1A1101247).

Conflicts of Interest: The authors declare no conflict of interest.

References

1. Zhang, J.; Zhao, X.S. On the Configuration of Supercapacitors for Maximizing Electrochemical Performance. *Chem. Sus. Chem.* **2021**, *5*, 818–841. [CrossRef] [PubMed]
2. Kou, T.; Yao, B.; Liu, T.; Li, Y. Recent advances in chemical methods for activating carbon and metal oxide based electrodes for supercapacitors. *J. Mater. Chem. A* **2017**, *5*, 17151–17173. [CrossRef]
3. Naoi, K.; Ishimoto, S.; Miyamoto, J.-I.; Naoi, W. Second generation 'nanohybrid supercapacitor': Evolution of capacitive energy storage devices. *Energy Environ. Sci.* **2012**, *5*, 9363–9373. [CrossRef]
4. Yan, J.; Wang, Q.; Wei, T.; Fan, Z. Recent advances in design and fabrication of electrochemical supercapacitors with high energy densities. *Adv. Energy Mater.* **2014**, *4*, 1300816. [CrossRef]
5. Bose, S.; Kuila, T.; Mishra, A.K.; Rajasekar, R.; Kim, N.H.; Lee, J.H. Carbon-based nanostructured materials and their composites as supercapacitor electrodes. *J. Mater. Chem.* **2012**, *22*, 767–784. [CrossRef]
6. Huang, Y.; Liang, J.; Chen, Y. An Overview of the Applications of Graphene-Based Materials in Supercapacitors. *Small* **2012**, *8*, 1805–1834. [CrossRef] [PubMed]
7. Wang, K.B.; Xun, Q.; Zhang, Q. Recent progress in metal-organic frameworks as active materials for supercapacitors. *Energy Chem.* **2020**, *2*, 100025. [CrossRef]
8. Wang, K.; Bi, R.; Huang, M.; Lv, B.; Wang, H.; Li, C.; Wu, H.; Zhang, Q. Porous Cobalt Metal–Organic Frameworks as Active Elements in Battery–Supercapacitor Hybrid Devices. *Inorg. Chem.* **2020**, *59*, 6808–6814. [CrossRef] [PubMed]
9. Park, S.K.; Mahmood, Q.; Park, H.S. Surface functional groups of carbon nanotubes to manipulate capacitive behaviors. *Nanoscale* **2013**, *5*, 12304–12309. [CrossRef] [PubMed]
10. Zhang, L.L.; Zhao, X.S. Carbon-based materials as supercapacitor electrodes. *Chem. Soc. Rev.* **2009**, *38*, 2520–2531. [CrossRef] [PubMed]
11. Dillon, A.C. Carbon Nanotubes for Photoconversion and Electrical Energy Storage. *Chem. Rev.* **2010**, *110*, 6856–6872. [CrossRef] [PubMed]
12. Frackowiak, E.; Béguin, F. Carbon materials for the electrochemical storage of energy in capacitors. *Carbon* **2001**, *39*, 937–950. [CrossRef]
13. Frackowiak, E. Carbon materials for supercapacitor application. *Phys. Chem. Chem. Phys.* **2007**, *9*, 1774–1785. [CrossRef] [PubMed]
14. Deng, W.; Ji, X.; Chen, Q.; Banks, C.E. Electrochemical capacitors utilising transition metal oxides: An update of recent developments. *RSC Adv.* **2011**, *1*, 1171–1178. [CrossRef]
15. Wang, C.; Xu, J.; Yuen, M.-F.; Zhang, J.; Li, Y.; Chen, X.; Zhang, W. Hierarchical composite electrodes of nickel oxide nanoflake 3D graphene for high-performance pseudocapacitors. *Adv. Funct. Mater.* **2014**, *24*, 6372–6380. [CrossRef]
16. Wang, Y.; Guo, J.; Wang, T.; Shao, J.; Wang, D.; Yang, Y.-W. Mesoporous Transition Metal Oxides for Supercapacitors. *Nanomaterials* **2015**, *5*, 1667–1689. [CrossRef] [PubMed]
17. Augustyn, V.; Simon, P.; Dunn, B. Pseudocapacitive oxide materials for high-rate electrochemical energy storage. *Energy Environ. Sci.* **2014**, *7*, 1597–1614. [CrossRef]
18. Lokhande, C.D.; Dubal, D.P.; Joo, O.-S. Metal oxide thin film based supercapacitors. *Curr. Appl. Phys.* **2011**, *11*, 255–270. [CrossRef]
19. Lee, S.-W.; Kim, H.-K.; Kim, M.-S.; Roh, K.C.; Kim, K.-B. A study of the effects of synthesis conditions on Li5FeO4/carbon nanotube composites. *Sci. Rep.* **2017**, *7*, 46530. [CrossRef]
20. Beyer, H.; Meini, S.; Tsiouvaras, N.; Piana, M.; Gasteiger, H.A. Thermal and electrochemical decomposition of lithium peroxide in non-catalyzed carbon cathodes for Li-air batteries. *Phys. Chem. Chem. Phys.* **2013**, *15*, 11025–11037. [CrossRef] [PubMed]
21. Dresselhaus, M.S.; Jorio, A.; Hofmann, M.; Dresselhaus, G.; Saito, R. Perspectives on Carbon Nanotubes and Graphene Raman Spectroscopy. *Nano Lett.* **2010**, *10*, 751–758. [CrossRef] [PubMed]
22. Berciaud, S.; Ryu, S.; Brus, L.E.; Heinz, T.F. Probing the Intrinsic Properties of Exfoliated Graphene: Raman Spectroscopy of Free-Standing Monolayers. *Nano Lett.* **2009**, *9*, 346–352. [CrossRef] [PubMed]
23. Sinan, N.; Unur, E. Fe_3O_4/carbon nanocomposite: Investigation of capacitive & magnetic properties for supercapacitor applications. *Mater. Chem. Phys.* **2016**, *183*, 571–579.
24. Yu, R.; Jiang, C.F.; Chu, W.; Ran, M.F.; Sun, W.J. Decoration of CNTs' surface by Fe_3O_4 nanoparticles: Influ-ence of ultrasonication time on the magnetic and structural properties. *Chin. Chem. Lett.* **2017**, *28*, 302–306. [CrossRef]

25. Guan, D.; Gao, Z.; Yang, W.; Wang, J.; Yuan, Y.; Wang, B.; Zhang, M.; Liu, L. Hydrothermal synthesis of carbon nanotube/cubic Fe_3O_4 nanocomposite for enhanced performance supercapacitor electrode material. *Mater. Sci. Eng. B* **2013**, *178*, 736–743. [CrossRef]
26. Kim, H.-K.; Roh, K.C.; Kim, K.-B. In Situ Electrochemical dilatometric study of Fe_3O_4/Reduced graphene oxide nanocomposites as anode material for lithium ion batteries. *J. Electrochem. Soc.* **2015**, *162*, A2308. [CrossRef]
27. Su, J.; Cao, M.; Ren, L.; Hu, C. Fe_3O_4–Graphene Nanocomposites with Improved Lithium Storage and Magnetism Properties. *J. Phys. Chem. C* **2011**, *115*, 14469–14477. [CrossRef]
28. Fu, C.; Zhao, G.; Zhang, H.; Li, S. A Facile Route to Controllable Synthesis of Fe_3O_4/Graphene Composites and Their Application in Lithium-Ion Batteries. *Int. J. Electrochem. Sci.* **2014**, *9*, 46–60.
29. Ghasemi, S.; Ahmadi, F. Effect of surfactant on the electrochemical performanceof graphene/iron oxide electrode for supercapacitor. *J. Power Sources* **2015**, *289*, 129–137. [CrossRef]
30. Kim, Y.H.; Park, S.J. Roles of nanosized Fe_3O_4 on supercapacitive properties of carbon nanotubes. *Curr. Appl. Phys.* **2011**, *11*, 462–466. [CrossRef]
31. Nawwar, M.; Poon, R.; Chen, R.; Sahu, R.P.; Puri, I.K.; Zhitomirsky, I. High areal capacitance of Fe_3O_4-decorated carbon nanotubes for supercapacitor electrodes. *Carbon Energy* **2019**, *1*, 124–133. [CrossRef]